

Roton-phonon mixing in solid hydrogen and deuterium

Ad Lagendijk and Rinke J. Wijngaarden

Natuurkundig Laboratorium, Universiteit van Amsterdam, Valckenierstraat 65, 1018 XE Amsterdam, The Netherlands

Isaac F. Silvera

Lyman Laboratory of Physics, Harvard University, Cambridge, Massachusetts 02138

(Received 16 July 1984)

Solid parahydrogen and orthodeuterium have been studied under high pressure in a diamond anvil cell at low temperature. The frequency of the $\vec{k}=0$ E_{2g} transverse-optical phonon increases rapidly with density. In the vicinity of the roton modes it hybridizes with the E_{2g} roton resulting in a level anticrossing. The interaction Hamiltonian is analyzed for an (effective) linear coupling between the roton and phonon. Of the two most important contributions to the coupling, the crystal-field interaction $B(R)$ is found to be significantly stronger than the mechanism arising from the electric quadrupole-quadrupole interaction $\Gamma(R)$. This enables us to make the first determination of $B(R)$ in the solids at two densities. The resulting experimental potential is significantly smaller than the theoretical pair potential. These measurements provide an important experimental test for theoretical anisotropic potentials.

I. INTRODUCTION

The even- J solids parahydrogen (p- H_2) and orthodeuterium (o- D_2) have well-defined rotational excitations which are called rotons.^{1,2} These excitations correspond to collective modes of the $J=2$ single-molecule rotational states. For the hcp structure, which has two sublattices, there are $2 \times (2J+1) = 10$ rotons at each wave vector \vec{k} , whose degeneracies can be partially lifted by anisotropic interactions between the molecules. These interactions split the Raman-active $\vec{k}=0$ rotons into three distinct levels characterized by J and its projection m ; $|J, m\rangle$: $|2, \pm 1\rangle$, $|2, \pm 2\rangle$, and $|2, 0\rangle$ in order of ascending energy. Since the splittings are due to anisotropic interactions, in principle the observation of these modes and the study of their behavior as a function of density should be very useful for determining the anisotropic interactions in these materials, and in particular for the potential between a pair of molecules. There is, however, one important interaction, the crystalline field $B(R)$, which due to the symmetry of the hcp lattice makes a negligible contribution to the roton energies. We will show that the roton-phonon mixing is largely determined by $B(R)$, and that our experimental study of the roton-phonon mixing in p- H_2 and o- D_2 provides us with values of $D(R)$:

$$D(R) \equiv \frac{dB(R)}{dR} - \frac{2B(R)}{R}$$

at two densities.

Recently the density dependence of the roton energies has been observed by Raman scattering in a high-pressure diamond anvil cell.³ Above a critical pressure of 278 kbar a phase transition to an orientationally ordered phase was observed in o- D_2 . Below this pressure, the low-lying rotational excitations from the ground state are the rotons. At much lower pressures the E_{2g} transverse-optical pho-

non crosses the roton band, where it hybridizes with the E_{2g} roton resulting in level repulsion. This was first reported for o- D_2 ,⁴ and later observed in p- H_2 .³ In this paper we will discuss the roton-phonon mixing in detail.

In Ref. 4 it was phenomenologically shown that the roton-phonon hybridization could be described by a linear coupling of the form $Ca^\dagger b$, where C is the coupling constant, and a^\dagger and b^\dagger are roton and phonon creation operators. Note the change in notation with respect to Ref. 4; this is done to comply with the conventional labeling of the modes. Here we present a microscopic analysis of the coupling and show that C mainly arises from the crystal-field anisotropic intermolecular interaction $B(R)$. A comparison between the experimental value and theoretical expression for C enables a determination of $D(R)$ at two densities. We find that the experimentally observed values for C are much smaller than the values calculated with theoretical potentials.

In Sec. II we briefly review the unperturbed roton and phonon and show the effect of the linear coupling on the spectrum. Experimental details are given in Sec. III. The contribution of single-particle interactions (crystal-field terms) to the roton-phonon mixing will be calculated in Sec. IV. In higher order, two-particle interactions also contribute to the roton-phonon coupling. In Sec. V we will consider the electrostatic quadrupole-quadrupole interaction (EQQ) and calculate the EQQ component to the roton-phonon mixing, and we will discuss briefly several other anisotropic two-particle interactions. Our conclusions can be found in Sec. VI.

II. INTERACTIONS, ROTONS AND PHONONS

The Hamiltonian for the solid hydrogens is

$$H = \sum_i \frac{P_i^2}{2M} + \sum_{ij} V_I(R_{ij}) + \sum_i B \vec{J}_i^2 + \sum_{ij} V_A(\vec{R}_{ij}, \Omega_i, \Omega_j). \quad (1)$$

Here the first term is the translational kinetic energy of the molecular centers with mass M , and the third term is the rotational kinetic energy where $B = \hbar/2I$ is the rotational constant and I is the moment of inertia; $B = 59.3 \text{ cm}^{-1}$ for H_2 and 29.9 cm^{-1} for D_2 . The intermolecular part is partitioned into an isotropic part, V_I , and an anisotropic part, V_A . In Eq. (1) \vec{R}_{ij} is the intermolecular vector between molecule i and j , and $\Omega_i \equiv \theta_i, \phi_i$ describes the orientation of molecule i with respect to a crystal-fixed reference frame. By writing the Hamiltonian in form (1) we have separated the terms associated with the phonon degrees of freedom [the first two terms in expression (1)] from the terms associated with the roton degrees of freedom.

We are interested in the two E_{2g} $\vec{k}=0$ phonons, which by standard techniques can be represented (ignoring zero-point energies) by

$$H_P = \hbar\omega_P (b_1^\dagger b_1 + b_{-1}^\dagger b_{-1}). \quad (2)$$

Here the subscripts 1, -1 designate polarizations, which will be described further on in the paper. The set of phonon creation operators $\{b_1^\dagger, b_{-1}^\dagger\}$ span the complex representation of E_{2g} .⁵ The phonon angular frequency ω_P is related in a complicated way to the mass and to V_I in a manner which is unimportant for the present discussion.⁶ We note that the mode Grüneisen constant

$$\gamma_{\text{TO}} = \frac{\partial \ln(\omega_P/\omega_P^0)}{\partial \ln(V/V_0)} \approx 2, \quad (3)$$

$$V_A(R_{ij}, \omega_i, \omega_j) = \left[\frac{16\pi}{5} \right]^{1/2} B(R_{ij}) [Y_2^0(\omega_i) + Y_2^0(\omega_j)] + \left[\frac{16\pi}{9} \right]^{1/2} A(R_{ij}) [Y_4^0(\omega_i) + Y_4^0(\omega_j)] \\ + 4\pi \sum_{J=0,2,4} \epsilon_J(R_{ij}) \beta_J \sum_m \begin{pmatrix} 2 & 2 & J \\ m & -m & 0 \end{pmatrix} Y_2^m(\omega_i) Y_2^{-m}(\omega_j). \quad (5)$$

Here $\begin{pmatrix} 2 & 2 & J \\ m & -m & 0 \end{pmatrix}$ is a 3-j symbol,⁹ $(\beta_J)^{-1} = \begin{pmatrix} 2 & 2 & J \\ 2 & -2 & 0 \end{pmatrix}$, and $Y_2^m(\omega_i)$ is a spherical harmonic with $\omega_i \equiv \theta_i, \phi_i$, the angles describing the orientation of the i th molecule with respect to the intermolecular axis. $B(R)$ (to be distinguished from the rotational constant B), $A(R)$, and $\epsilon_J(R)$ describe the radial dependences of the interactions. Note that in problems where more than two molecules are involved (such as the solid) it is very useful to transform expression (5) to a reference frame which is fixed in space and the same for all molecules. This can be done in a straightforward way by using Wigner rotation matrices.⁹ It was this form of V_A that was used in Eq. (1).

The term involving $B(R)$ is an effective single-particle interaction, and is usually referred to as the crystal-field term in solid-state problems. In a crystal-fixed reference frame this interaction is given by

$$V_{2c}(i) = (8\pi/5) \sum_{j,m} Y_2^m(\Omega_i) B(R_{ij}) Y_2^m(\hat{R}_{ij})^*, \quad (6)$$

where we sum over neighbors j .

Here R_{ij} is the distance between molecule i and j , and

so that the phonon frequency has a strong density dependence.⁷ In Eq. (3) ω_P^0 refers to the zero-pressure phonon angular frequency and V_0 refers to the zero-pressure molar volume.

Let us define the lattice displacement operator $\vec{u}(j\gamma) \equiv \vec{R}_{i\beta, j\gamma} - \vec{R}_{i\beta, j\gamma}^0$, in which $\vec{R}_{i\beta, j\gamma}$ refers to the position of the molecule at lattice cell j and sublattice γ with respect to reference site (i, β) . The superscript 0 on the lattice vectors, $\vec{R}_{i\beta, j\gamma}^0$, indicates the static equilibrium lattice vectors. We expand the lattice displacements in phonon coordinates by using the standard phonon expansion⁸ and by singling out the $\vec{k}=0$ E_{2g} contribution, arriving at

$$u_\epsilon(j\gamma) - u_\epsilon(i\beta) = (\hbar/NM\omega_P)^{1/2} (b_\epsilon + b_{-\epsilon}^\dagger) \delta_{\gamma, -\beta}, \quad \epsilon = \pm 1 \quad (4)$$

where we ignore $\vec{k} \neq 0$ contributions. Here ϵ refers to complex Cartesian components [$\epsilon = \pm 1 \rightarrow (\mp 1/\sqrt{2})(x \pm iy)$, $\epsilon = 0 \rightarrow z$]. In Eq. (4) N is the number of unit cells. The E_{2g} phonons do not involve displacements along the z (hexagonal axis) direction.

For the roton modes the anisotropic potential V_A , which includes single-particle interactions, is very important. Both the roton energies and the roton-phonon coupling are to a large degree determined by V_A . A general form of the anisotropic interaction between two molecules is given by^{1,2}

$\hat{R}_{ij} \equiv \vec{R}_{ij}/R_{ij}$ describes the orientation of the intermolecular axis with respect to the hcp crystal axes. The orientation of molecule i with respect to the crystal frame is given by Ω_i . For a perfect hcp lattice without zero-point motion the summation over the first two shells of the right-hand side of Eq. (6) vanishes. This is due to a symmetry property of the hcp lattice which in Griffith's terminology would be referred to as "intermediate symmetry."¹⁰ Van Kranendonk and Sears¹¹ and Luryi and Van Kranendonk¹² have shown that zero-point motion gives rise to a nonvanishing of the crystal-field interaction in the hcp lattice. Nevertheless, it is quite small, of order $10^{-2} - 10^{-3} \text{ cm}^{-1}$ at zero pressure. Although the radial strength factor $B(R)$ can be quite large ($\sim 1 \text{ cm}^{-1}$ at zero pressure increasing rapidly with density), due to the cancellation of the angular factors in Eq. (6), the crystal field itself hardly affects the roton spectrum and is quite difficult to determine experimentally. We shall see later that the crystal-field interaction of rank four, that is the term in Eq. (5) proportional to $A(R)$ does not contribute to the roton-phonon coupling.

Of the two-particle interactions in Eq. (5) the EQQ coupling, which is included in the $J=4$ operator in Eq. (5), is dominant at zero pressure and is expected to remain so throughout the pressure range studied here. Its strength is often represented in terms of the EQQ coupling parameter $\Gamma(R) \equiv \frac{6}{25} e^2 Q^2 / R^5$ in which Q is the EQ moment of the molecule. If the $J=4$ component consists solely of the EQQ interaction, $\epsilon_4(R) = \frac{5}{6} \Gamma(R)$. In H_2 $\Gamma(R_0) = 0.66 \text{ cm}^{-1}$ and in D_2 $\Gamma(R_0) = 0.82 \text{ cm}^{-1}$, in which R_0 refers to the zero-pressure lattice constant. These are "bare" zero-pressure values; the actual zero-pressure values will be renormalized considerably by the zero-point motion.¹³ At low pressures it is often sufficient to limit the anisotropic interactions to EQQ to determine the energies.

We will now discuss the eigenvalue problem associated with the rotational part of Eq. (1). At low pressures the single-particle states are well described by free-rotor states $|Jm\rangle$. Due to the anisotropic two-particle interactions, the low-lying $J=2$ roton excitations are of a collective (exciton) nature. At any wave vector \vec{k} we have ten rotors resulting from the fivefold degenerate $J=2$ level and from the two-sublattice structure. Recently a very convenient second-quantization formalism was introduced to describe the low-lying rotational excitations.¹⁴ In this formalism $\{a_{i,m}^\dagger, a_{i,m}\}$ are the creation and destruction operators of the m th dimension of a five-dimensional oscillator at site i . A very important operator equivalent for tensors of rank two, $Y_2^m(\Omega_i)$, in this representation is

$$Y_2^m(\Omega_i) = (4\pi)^{-1/2} [a_{i,m}^\dagger + (-1)^m a_{i,-m}] + \sum_{m'} A(m, m' - m) a_{i,m}^\dagger a_{i,m' - m}, \quad (7a)$$

in which $A(m, m' - m)$ is a function of 3- j symbols,

$$A(m, m' - m) = (-1)^{m'+1} 5(14\pi)^{-1/2} \begin{pmatrix} 2 & m & 2 \\ m' & m' - m & -m \end{pmatrix}. \quad (7b)$$

In Eq. (7a) some unimportant projection operators are omitted. The roton excitations can be characterized by introducing the wave-vector-dependent operators $\{a_{m,\alpha}(\vec{k}), a_{m,\alpha}^\dagger(\vec{k})\}$, where α indicates one sublattice and $-\alpha$ the other sublattice. We are interested in the Raman-active E_{2g} modes:

$$a_1 \equiv (2)^{-1/2} [a_{2,\alpha}(\vec{k}=0) + a_{2,-\alpha}(\vec{k}=0)], \quad (8a)$$

$$a_{-1} \equiv (2)^{-1/2} [a_{-2,\alpha}(\vec{k}=0) + a_{-2,-\alpha}(\vec{k}=0)]. \quad (8b)$$

The set of destruction operators $\{a_1, a_{-1}\}$ span the complex representation of E_{2g} .⁵ The harmonic part of the Hamiltonian of these rotors can be written as

$$H_R = \hbar\omega_R (a_1^\dagger a_1 + a_{-1}^\dagger a_{-1}), \quad (9)$$

where ω_R includes the rotational kinetic- and potential-energy contributions. The theoretical determination of ω_R at high density is rather involved. The best solution so far was given by Lagendijk and Silvera,¹⁴ who diagonalized all the quadratic terms in the roton Hamiltonian by a suitable Bogoliubov transformation. Roton anharmonicities have been included recently.¹⁵ For the present paper it is, however, sufficient to use the experimental

values of ω_R . Since the major part of the anisotropic interactions are traceless, only the splitting of the roton bands will increase rapidly with density and the center of gravity will depend rather weakly on density. This behavior should be contrasted with the phonon, the excitation energy of which depends strongly on density, and as a result by varying the external pressure the phonons will cross the rotors.

In this paper we show that $B(R)$ is responsible for the mode anticrossing and can thus be experimentally determined. At the point of crossing of rotors and phonons the roton-phonon coupling will become very important for the mode energies. The E_{2g} roton and E_{2g} phonon have the same symmetry, and a linear interaction of the form

$$H_I = \hbar C (a_1^\dagger b_1 + a_{-1}^\dagger b_{-1}) + \text{H.c.}, \quad (10)$$

is allowed by symmetry. The coupling coefficient C will be density dependent. The experiments on the roton-phonon mixing will be explained on the basis of the following Hamiltonian

$$H = H_P + H_R + H_I. \quad (11)$$

This Hamiltonian is easily diagonalized and the resulting excitation frequencies are given by

$$\omega = \frac{1}{2} (\omega_R + \omega_P) \pm \frac{1}{2} [\omega_R - \omega_P]^2 + 4C^2]^{1/2}. \quad (12)$$

The two unperturbed modes are now hybridized and are phononlike and rotonlike far from the anticrossing. By fitting the experimental spectra to Eq. (12), the coupling constant C can be determined. It is straightforward to calculate the relative intensities of the two modes in Raman scattering taking the mixing into account.¹⁶

III. EXPERIMENTAL OBSERVATIONS

Samples of 98.5 mol % p- H_2 and 98.5 mol % o- D_2 were prepared by catalytic conversion in the liquid state. Pressure was applied in our diamond anvil cell, with a pressure range up to 600 kbar. The cell is positioned in a ^4He cryostat enabling temperature control in the range 1.1–300 K. Samples were confined in a steel T 301 gasket; typical sample size was 100 μm in diameter and about 10–20 μm thick. Present experimental data were obtained in several runs on both isotopes. The excitations were observed in a Raman backscattering geometry. An argon-ion laser with power up to 300 mW in the 5145- \AA line was employed. Pressure was determined from the luminescence spectrum of a few grains of ruby, enclosed with the sample, which was also excited by the laser. The pressure calibration of Mao *et al.*¹⁷ was used. At the beginning of each experimental run the zero-pressure frequency of the fluorescence line was determined at 5 K. This zero-pressure frequency was used when applying Mao *et al.*'s formula.

We have studied the $E_{2g}(|2, \pm 2\rangle)$ roton and the E_{2g} transverse-optical phonon at 5 K. The pressure dependence of the frequency is plotted in Fig. 1. Frequency is plotted as a function of absolute density which allows for easy comparison between hydrogen and deuterium. To

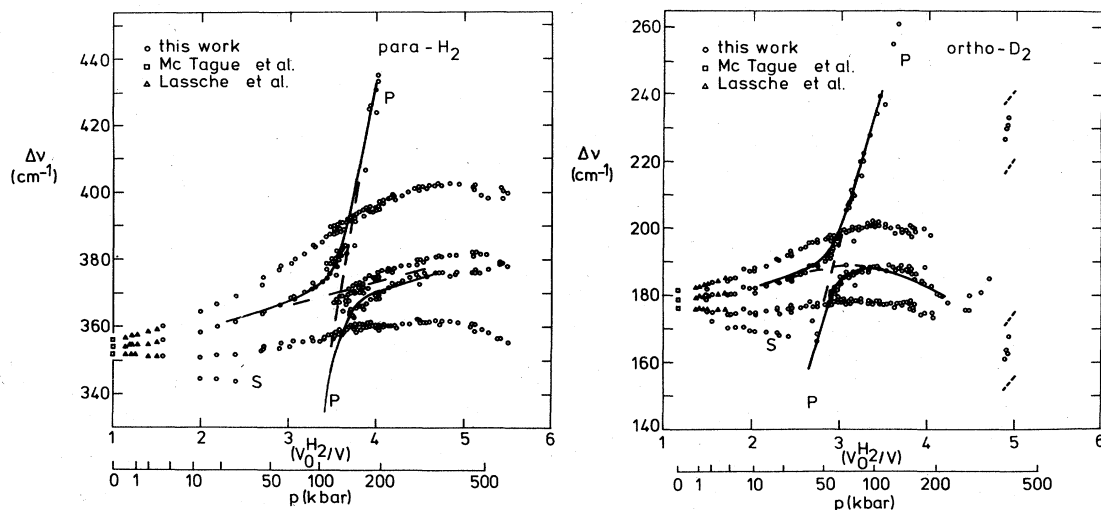


FIG. 1. Roton and phonon (P) data, plotted against absolute density [scaled to the zero-pressure density of hydrogen, $(V_0^2)^{-1}$] to allow for easy comparison of the H_2 and D_2 data. Low-pressure points are from Bhatnager *et al.* (Ref. 18), McTague *et al.* (Ref. 19), and Lassche *et al.* (unpublished).

provide a common dimensionless scale we divided the density by the zero-pressure density of hydrogen. The bending over in D_2 at ≈ 100 kbar and at H_2 at ≈ 400 kbar and also the severe line broadening in D_2 above 160 kbar are considered to be precursors to the phase transition into the librating phase.³ Pressure was determined with an accuracy of 1 kbar. The accuracy in the frequency determination was 0.2 cm^{-1} , whereas the reproducibility between different runs was about 1 cm^{-1} within 60% confidence limits in the high-pressure regime.

After initial loading of the sample and compression up to 2–10 kbar often a roton spectrum consisting of four lines was observed. In Fig. 1 the extra line is labeled S . After annealing the sample at about one-half of the melting temperature, a three-line spectrum was always observed. Because of this we believe that the effect is caused by strain due to nonhydrostatic compression of the sample.⁴ Our samples were always annealed below 40 kbar, and nearly all our samples and particularly those used for the highest pressures were frequently annealed at 80 K and sometimes even at 300 K.

In this paper we want to focus on the roton-phonon mixing which occurs for the E_{2g} excitations. It is clear that the mixing can be described by a formula such as Eq. (12), and therefore we are observing an (effective) linear

coupling between the roton and phonon. Fitting the data of Eq. (12) results in the following values for the coupling constant at the densities of the mixing: for deuterium, $C/2\pi c = 6 \pm 1 \text{ cm}^{-1}$ at $V = 7.92 \text{ cm}^3/\text{mol}$; and for hydrogen, $C/2\pi c = 12 \pm 2 \text{ cm}^{-1}$ at $V = 6.41 \text{ cm}^3/\text{mol}$ (c being the speed of light). A summary of the parameters at the crossing is given in Table I. Due to problems with background fluorescence the phononlike branches have been measured mostly where their frequency exceeds the frequency of the highest roton branch. In Fig. 2 we present some data on the relative intensity of the E_{2g} phononlike excitation and the E_{2g} rotonlike excitation. Experimentally it is difficult to determine the absolute intensity of the phononlike branch because the intensity of the middle roton enters into it and the middle roton exchanges intensity with the other two roton branches if the orientations

TABLE I. Parameters at the roton-phonon crossing.

	H_2	D_2	Units
p	130.6	53.1	kbar
V	6.41	7.92	cm^3/kbar
R	2.47	2.65	\AA
R	4.67	5.01	bohrs
ω_p	369	187	cm^{-1}
$\Gamma_{NN}(R)$	5.6	3.8	cm^{-1}
m	2	4	relative
$C/2\pi c - \text{exp}$	12 ± 2	6 ± 1	cm^{-1}

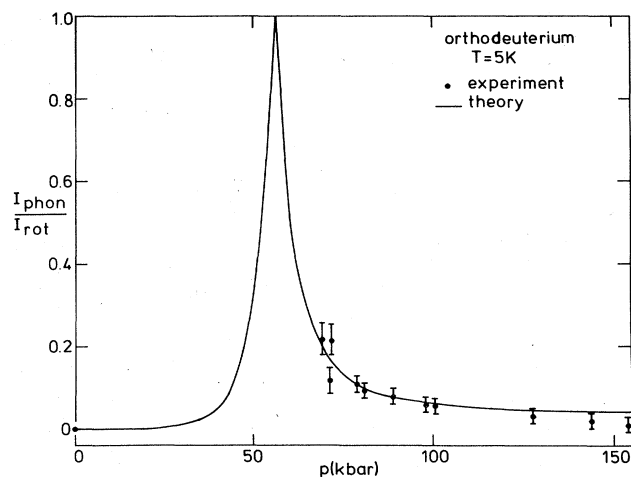


FIG. 2. Intensity ratio of phononlike to rotonlike excitations. The zero-pressure point is by Silvera *et al.* (Ref. 20). The theoretical description is discussed in Sec. IV.

of the crystallites change when pressure is changed in the sample (we have experimental indication that this does happen).

The theoretical curve in Fig. 2 for the relative intensity of the rotonlike and phononlike excitations was obtained by diagonalization of $H = H_P + H_R + H_I$.¹⁶

IV. THE CRYSTAL-FIELD INTERACTION

The source of the roton-phonon coupling is not *a priori* clear and must be determined by detailed evaluation. This is done by expanding V_A around the rigid lattice in phonon coordinates. Although the EQQ interaction is dominant, the linear roton-phonon coupling only arises from this interaction in second-order perturbation theory, whereas a first-order term is present in the crystal-field term V_{2c} . We shall compare these two contributions.

An expansion of the displacement field around the static lattice of V_{2c} provides a linear coupling. The interaction V_{2c} for a static hcp lattice is extremely small due to the cancellation of angular factors. For the roton-phonon mixing one is interested in the dynamic coupling to the phonons, and all crystal-field components, including those with a vanishing average for the static lattice, should be considered. An analogous situation exists for the crystal-field splitting of the $J=1$ level of an o- H_2 impurity in a p- H_2 matrix.¹² Introduction of the operator equivalent (7a) in Eq. (6) and expanding in powers of the displacement generates a linear roton-phonon coupling. In Fig. 3 we give a schematic diagram of the crystal-field contribution. This linear term is given by

$$V_{2c}^{RP} = (8\pi/5) \sum_{j,m} \{ Y_2^m(\Omega_i) \vec{\nabla} [B(R_{ij}) Y_2^m(\hat{R}_{ij})^*] \cdot [\vec{u}(j) - \vec{u}(i)] \} \quad (13)$$

Using the gradient formula⁹

$$\nabla_{\pm 1} Y_2^{\pm 2}(\hat{R}) f(R) = \frac{1}{2} \left[\frac{df(R)}{dR} - \frac{2}{R} \right] Y_3^{\pm 3}(\hat{R}), \quad (14)$$

in Eq. (13) and substitution of the phonon expansion (4) in Eq. (13) gives the roton-phonon coupling in form (10). Summing the crystal field over nearest neighbors, we find the following expression for the roton-phonon splitting,

$$|C|/2\pi c = 0.633(\hbar/M\omega_p)^{1/2} |D(R_{NN})|, \quad (15a)$$

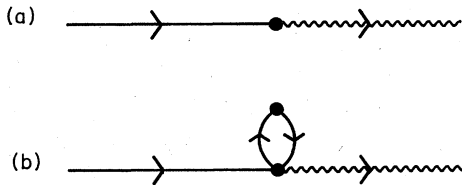


FIG. 3. Schematic diagrammatic representation of the roton-phonon coupling. Wavy lines represent phonons, solid lines represent rotors. No wave-vector and angular momentum labels are shown. (a) Vertex symbolizes crystal-field interaction; (b) vertices symbolize EQQ interaction.

in which

$$D(R) \equiv \frac{dB(R)}{dR} - \frac{2B(R)}{R}, \quad (15b)$$

and where R_{NN} is the nearest-neighbor distance. Evaluating $D(R_{NN})$ for some model potentials demonstrates that at the density where the mixing occurs the approximation of restricting the interactions to nearest neighbors is a very good one.

If the roton-phonon mixing would only be due to the crystal-field interaction, the experimental data would provide us with an accurate determination of $D(R_{NN})$ and therefore of $B(R_{NN})$. We have evaluated the crystal-field contribution for three recent *ab initio* calculations of the H_2 pair potential by Ree and Bender,²¹ Burton and Senff,²² and Meyer and Schaefer.²³ For (H_2, D_2) we find values (24,12), (28,15), and (24,13), respectively, all in units cm^{-1} , to be compared with the experimental values $(12 \pm 2, 6 \pm 1)$, all evaluated at the crossing density (see Table I). As stated earlier other experimental data such as the roton energies are insensitive to $B(R)$ because these experiments sample combinations of $B(R)Y_2^m(\hat{R})$, which vanish for the first few shells of an hcp lattice. We will now show that other sources to the roton-phonon mixing can be excluded.

The crystal-field term V_{4c} corresponding to the term with factor $A(R_{ij})$ in Eq. (5) must also be considered. The spherical harmonics of rank 4 which occur in V_{4c} do not have direct matrix elements between the rotator ground state and the $J=2$ excited state, and consequently V_{4c} does not contribute to the linear roton-phonon coupling. In the following section we consider two-particle interactions.

V. EQQ AND OTHER TWO-PARTICLE INTERACTIONS

The dominant anisotropic two-particle interaction is the EQQ coupling. This interaction was already discussed in Sec. II and this interaction was included in Eq. (5) where a general form of V_A was introduced. In solid-state problems it is more useful to describe spherical harmonics with respect to a crystal-fixed reference frame. By using this frame the EQQ coupling can be written

$$V_{\text{EQQ}} = \frac{1}{2} \sum_{i \neq j} \sum_{mn} D^{mn}(\vec{R}_{ij}) Y_2^m(\Omega_i) Y_2^n(\Omega_j), \quad (16a)$$

where

$$D^{mn}(\vec{R}_{ij}) = \frac{20}{3} (\pi)^{3/2} (70)^{1/2} \begin{bmatrix} 2 & 2 & 4 \\ m & n & -m-n \end{bmatrix} \times \Gamma(R_{ij}) Y_4^{-m-n}(\hat{R}_{ij}). \quad (16b)$$

Inserting operator equivalent (7) in Eq. (16) generates quadratic terms in boson operators and higher-order anharmonicities. Of all the anharmonicities only the cubic anharmonicity,

$$V_3 = \sum_{i \neq j} \sum_{mnm'} (4\pi)^{-1/2} A(n, m') D^{mn}(\vec{R}_{ij}) \times a_{i,m}^\dagger a_{j,m'+n}^\dagger a_{j,m'} + \text{H.c.} \quad (17)$$

generates a linear roton-phonon coupling in lowest order of $\Gamma(R_{NN})/B$. A complete analysis of the anharmonic terms, including their influence on the $\vec{k}=0$ roton energies and their effect on the soft rotors will be published elsewhere.¹⁵ Simplifying V_3 by introducing the Hartree approximation

$$\begin{aligned} a_{i,m}^\dagger a_{j,m'+n}^\dagger a_{j,m'} &\simeq \langle a_{i,m}^\dagger a_{j,m'+n}^\dagger \rangle a_{j,m'} \\ &\quad + \langle a_{i,m}^\dagger a_{j,m'} \rangle a_{j,m'+n} \\ &\quad + \langle a_{j,m'+n} a_{j,m'} \rangle a_{i,m}^\dagger \\ &\simeq (-12B)^{-1} (4\pi)^{-1} D^{m,m'+n}(\vec{R}_{ij})^* a_{j,m'}, \end{aligned} \quad (18a)$$

$$(18b)$$

in which Eq. (18b) was obtained by evaluating (18a) to lowest order in $\Gamma(R_{NN})/B$ at 0 K.

We find

$$V_3 = (4\pi)^{-3/2} (-12B)^{-1} \times \sum_{i \neq j} \sum_{mnm'} [D^{mn}(\vec{R}_{ij}) D^{m,m'+n}(R_{ij})^* a_{j,m'} + \text{H.c.}] \quad (19)$$

Expanding $D^{mn}(R_{ij})$ around $D^{mn}(R_{ij}^0)$ gives a term V'_3 , which is linear in the roton-phonon coupling,

$$V'_3 = 2(4\pi)^{-3/2} (12B)^{-1} \times \sum_{i \neq j} \sum_{mnm'} \{D^{mn}(R_{ij}^0) \vec{\nabla} D^{m,m'+n}(R_{ij}^0) \cdot [\vec{u}(j) - \vec{u}(i)] a_{j,m} + \text{H.c.}\} \quad (20)$$

Insertion of phonon expansion (4) in Eq. (20) and use of the gradient formula

$$\nabla_\mu Y_4^m(\hat{R}) R^{-5} = 9(-1)^{\mu+m} 5^{1/2} \binom{5}{-\mu-m} \binom{1}{\mu} \binom{4}{m} Y_5^{m+\mu} R^{-6} \quad (21)$$

produces a linear roton-phonon coupling of form (10).

Due to the strong R -dependence of the lattice sums in Eq. (20), $\propto R^{-11}$, it is more than sufficient to sum over nearest neighbors only. After some algebra we find

$$|C|/2\pi c = 15.66 (\hbar/M\omega_p)^{1/2} B^{-1} (\Gamma_0^2/R_0)(R_0/R_{nm})^{11}, \quad (22)$$

in which $\Gamma_0 \equiv \Gamma(R_0)$. Evaluating $|C|/2\pi c$ at the density of the mixing, we find 0.68 cm^{-1} for H_2 and 0.60 cm^{-1} for D_2 , which should be compared with the experimental values of 12 cm^{-1} and 6 cm^{-1} , respectively. The relative

sign of the crystal-field contribution and the EQQ component is such that they tend to work against each other. If we would like to extend our calculation to higher order in $\Gamma(R_{NN})/B$ we are faced with an enormous task, because the computations should not be done in real space any longer. We have to diagonalize a nontrivial non-Hermitean Bogoliubov matrix of 20×20 at each \vec{k} .^{24,25} Care should be taken to rearrange all anharmonicities, because the Bogoliubov transformation mixes the creation and destruction operators. Given our rather meager understanding of the density dependence of the total anisotropic potential this formidable calculation is not worth pursuing. The corrections to our perturbation results are estimated to be at most 30% and may well be such that the total EQQ contribution is less than result (22). Contrary to the crystal-field case a larger EQQ interaction has very severe consequences for the roton energies, and this possibility to obtain a larger roton-phonon mixing term can be excluded on those grounds. The only two-particle interaction which could be considered without conflicting too much with the roton energies is the ϵ_0 component of Eq. (5).²⁶ However, a closer inspection of this interaction shows that it does not couple to the E_{2g} phonon at all. In Fig. 3 we have given a schematic diagram of the EQQ contribution to the roton-phonon coupling.

VI. CONCLUSIONS

We have evaluated several contributions to the roton-phonon mixing in the solid hydrogens. We conclude that the coupling parameter C is determined principally by the crystal field at these high densities. Other interactions, including the EQQ coupling give rise to minor contributions to the roton-phonon coupling. Using recent *ab initio* pair potentials we find that the experimentally determined crystal-field potential is softer than the theoretical ones: C calculated with *ab initio* potentials is about 2 times larger than experiment. Before we discuss possible origins of the disagreement between theory and experiment we should point out that the experiment essentially probes $dB(R)/dR$ rather than $B(R)$ itself. It is quite possible that the theories provide realistic values for $B(R)$ but less reliable values for $dB(R)/dR$. The experiment should be considered as an extreme stringent test of the theory.

We believe that the discrepancy between theory and experiment has two origins other than limitations of theory due to the use of limited basis sets. The theoretical calculations of the molecular interaction are carried out for a fixed number of orientations of the molecular axes, usually five or six. The anisotropic potential of the form $V_I + V_A$ [see Eq. (1)] is then fit for this finite number of orientations. This limits the number terms in the expansion. Since the expansion is not complete, if an important term is omitted, then the other terms will be affected. For example, in all theoretical potentials the term $A(R)$ of Eq. (5) has been omitted for no *a priori* reason. We recommend that theoretical calculations should be carried out for an additional one or two configurations to resolve this problem. A second source of difficulty in comparing solid-state experiments to pair potentials is that in the ex-

periment many-body forces will certainly become more important at higher densities.²⁷ The discrepancies between theory and experiment point to the difficulty in predicting the pressure of the transition to the high-density orientationally ordered phases³ of p-H₂ and o-D₂, based on the theoretical intermolecular potential of H₂.

ACKNOWLEDGMENTS

We gratefully acknowledge the Stichting voor Fundamenteel Onderzoek der Materie (FOM) for support. One of us (I.F.S.) also thanks the National Science Foundation (NSF), Contract No. DMR-82-13662 for support.

-
- ¹J. Van Kranendonk, *Physica (Utrecht)* **25**, 1080 (1959); J. Van Kranendonk and G. Karl, *Rev. Mod. Phys.* **40**, 531 (1968).
- ²For a general introduction, see I. F. Silvera, *Rev. Mod. Phys.* **52**, 393 (1980).
- ³I. F. Silvera and R. J. Wijngaarden, *Phys. Rev. Lett.* **47**, 39 (1981).
- ⁴R. J. Wijngaarden and I. F. Silvera, *Phys. Rev. Lett.* **44**, 456 (1980).
- ⁵J. S. Griffith, *The Irreducible Tensor Method For Molecular Symmetry Groups* (Prentice-Hall, London, 1962).
- ⁶V. V. Goldman, *J. Low Temp. Phys.* **38**, 149 (1980).
- ⁷P. J. Berkhout and I. F. Silvera, *J. Low Temp. Phys.* **36**, 231 (1979).
- ⁸A. A. Maradudin, in *Dynamical Properties of Solids*, edited by G. K. Horton and A. A. Maradudin (North-Holland, Amsterdam, 1974), Vol. 1.
- ⁹A. R. Edmonds, *Angular Momentum in Quantum Mechanics* (Princeton University, Princeton, 1960).
- ¹⁰J. S. Griffith, *Mol. Phys.* **8**, 217 (1964).
- ¹¹J. Van Kranendonk and V. F. Sears, *Can. J. Phys.* **44**, 313 (1966).
- ¹²S. Luryi and J. Van Kranendonk, *Can. J. Phys.* **57**, 933 (1979).
- ¹³V. V. Goldman, *Phys. Rev. B* **20**, 4478 (1979).
- ¹⁴A. Lagendijk and I. F. Silvera, *Phys. Lett.* **84A**, 28 (1981).
- ¹⁵J. Igarishi, *J. Phys. Soc. Jpn.* **53**, 2629 (1984).
- ¹⁶R. J. Wijngaarden, Ph.D. thesis, University of Amsterdam, 1982 (unpublished).
- ¹⁷H. K. Mao, P. H. Bell, J. W. Shaner, and D. J. Steinberg, *J. Appl. Phys.* **49**, 3276 (1978).
- ¹⁸S. S. Bhatnagar, E. J. Allin, and H. L. Welsh, *Can. J. Phys.* **40**, 9 (1962).
- ¹⁹J. P. McTague, I. F. Silvera, and W. N. Hardy, *Proceedings of the 2nd International Conference on Light Scattering in Solids, Paris, France, 1971* (Flammarion Sciences, Paris, 1972), p. 456.
- ²⁰I. F. Silvera, W. N. Hardy, and J. P. McTague, *Phys. Rev. B* **5**, 1578 (1972).
- ²¹F. H. Ree and C. F. Bender, *J. Chem. Phys.* **71**, 5362 (1979). We have fitted their results to the same spherical-harmonics decomposition as used in Refs. 22 and 23.
- ²²P. G. Burton and U. E. Senff, *J. Chem. Phys.* **76**, 6073 (1982).
- ²³J. Schaefer and W. Meyer, *J. Chem. Phys.* **70**, 344 (1979); we used the corrected values as given by W. Meyer and J. Schaefer (unpublished).
- ²⁴J. H. P. Colpa, *Physica (Utrecht)* **93A**, 327 (1978).
- ²⁵C. F. Coll, III and A. B. Harris, *Phys. Rev. B* **4**, 2781 (1971).
- ²⁶J. Van Kranendonk, *Can. J. Phys.* **38**, 240 (1960).
- ²⁷F. H. Ree and C. F. Bender, *Phys. Rev. Lett.* **32**, 85 (1974).